Brain Dynamics Based Automated Epileptic Seizure Detection

by

Vinay Venkataraman

A Thesis Presented in Partial Fulfillment
of the Requirements for the Degree
Master of Science

Approved April 2012 by the
Graduate Supervisory Committee:

Leonidas Jassemidis, Co-Chair
Andreas Spanias, Co-Chair
Konstantinos Tsakalis

ARIZONA STATE UNIVERSITY

May 2012

ABSTRACT

Approximately 1% of the world population suffers from epilepsy. Continuous long-term electroencephalographic (EEG) monitoring is the gold-standard for recording epileptic seizures and assisting in the diagnosis and treatment of patients with epilepsy. However, this process still requires that seizures are visually detected and marked by experienced and trained electroencephalographers. The motivation for the development of an automated seizure detection algorithm in this research was to assist physicians in such a laborious, time consuming and expensive task. Seizures in the EEG vary in duration (seconds to minutes), morphology and severity (clinical to subclinical, occurrence rate) within the same patient and across patients. The task of seizure detection is also made difficult due to the presence of movement and other recording artifacts. An early approach towards the development of automated seizure detection algorithms utilizing both EEG changes and clinical manifestations resulted to a sensitivity of 70-80% and 1 false detection per hour. Approaches based on artificial neural networks have improved the detection performance at the cost of algorithm's training. Measures of nonlinear dynamics, such as Lyapunov exponents, have been applied successfully to seizure prediction. Within the framework of this MS research, a seizure detection algorithm based on measures of linear and nonlinear dynamics, i.e., the adaptive short-term maximum Lyapunov exponent ($ASTL_{max}$) and the adaptive Teager energy (ATE) was developed and tested. The algorithm was tested on long-term

(0.5-11.7 days) continuous EEG recordings from five patients (3 with intracranial and 2 with scalp EEG) and a total of 56 seizures, producing a mean sensitivity of 93% and mean specificity of 0.048 false positives per hour. The developed seizure detection algorithm is data-adaptive, training-free and patient-independent. It is expected that this algorithm will assist physicians in reducing the time spent on detecting seizures, lead to faster and more accurate diagnosis, better evaluation of treatment, and possibly to better treatments if it is incorporated on-line and real-time with advanced neuromodulation therapies for epilepsy.

DEDICATION

To My Parents

ACKNOWLEDGMENTS

There are many individuals who have contributed towards this thesis. First, I would like to thank Dr. Leon for showing confidence in me and giving me an opportunity to work in his lab and on this project. His knowledge and support kept my research focused.

I would like to thank Dr. Andreas Spanias for being my co-chair and Dr. Konstantinos Tsakalis for serving as my committee member. I also sincerely thank Dr. Artemiadis Panagiotis for serving as a representative for my co-chair.

I am thankful to Dr. Ioannis Vlachos for guiding me throughout the project, development of algorithm and writing this thesis. I would like to thank Aaron Faith and Dr. Balu Krishnan for introducing me to EEG signal and epilepsy research. I would also like to thank Viju and all my friends for their continuous support.

TABLE OF CONTENTS

Page

LIST OF TABLES vii

LIST OF FIGURES viii

CHAPTER

1. INTRODUCTION 1

1.1. Overview 1

1.2. Electroencephalography 3

1.3. Classification of Epileptic Seizures 6

1.4. Brain Dynamics 10

1.5. Research Objectives 11

1.6. Thesis Organization 12

2. METHODS AND TOOLS 14

2.1. Dynamical Systems and Chaos 14

2.2. State Space Representation and State Space Reconstruction 18

2.3. Lyapunov Exponents 21

2.4. Teager Energy 23

2.5. Autocorrelation Function 24

2.6. Ictal vs Inter-ictal EEG 25

2.7. Adaptive Lyapunov exponents 27

2.8. Adaptive Teager Energy 28

3. SEIZURE DETECTION 31

3.1. Background 31

CHAPTER Page

3.2. Seizure Detection Algorithm 33

3.3. Example of Application of Seizure Detection Algorithm 38

4. APPLICATION TO SCALP AND INTRACRANIAL EEG 40

4.1. EEG Data Acquisition 40

4.2. Evaluation Procedure of Seizure Detection Algorithm 42

4.3. Case Analysis: Patient-3 43

4.4. Results 46

4.5. Full Comparison 47

5. CONCLUSION 50

REFERENCES 51

LIST OF TABLES

Table		Page
2.1	Analysis of Ictal vs Inter-ictal EEG (30sec with sub-band frequencies) ..	26
2.2	Analysis of ictal and inter-ictal EEG (with all frequencies)	26
4.1	Patient Data	42
4.2	Performance of Seizure Detection Algorithm	46
4.3	Performance of seizure detection algorithm for different combination of features for Patient-3 (Intracranial EEG recording) with mean performance across patients	49

LIST OF FIGURES

Figure Page

1. 1 90sec of intracranial EEG with a secondarily generalized complex partial seizure clinical seizure. Seizure onset is the right hippocampus.. 9

1.2 90sec of EEG with a simple partial sub-clinical seizure.. 9

2.1 Lorenz system: Trajectories in the state space with initial conditions x(0)=1, y(0)=2 and z(0)=3 and parameters σ=10, b=8/3, r=28 and N=20400..... 18

2.2 State space reconstruction of EEG data by the method of delays 23

2.3 Teager Energy for 10minutes of EEG from electrode RD4 in Patient-3 that includes a seizure: (a) Sample EEG with a seizure at 300sec (blue). (b) $ASTL_{max}$ values (black) estimated every 10 sec(c) ATE values (green) estimated every 10 sec 29

3.1 Flowchart of Seizure Detection Algorithm 37

3.2 Flow of seizure detection algorithm: (a) ASTLmax values for 1 hour of EEG recording from 4 electrodes. (b) ASTLmax values of selected electrode (Electrode-2) with threshold Th1. (c) ATE values of Electrode-2 with threshold Th2. (d) 21 ATE values of Electrode-2 corresponding to peak (marked as True detection in green) in (c). Seizures are announced if outliers occur at the same time in both Figures 3.2(c) and 3.2(d) 39

4.1 Electrode montage for intracranial and scalp EEG recording: (a) Placement of depth and subdural electrodes. Electrode strips placed over the left orbitofrontal (LOF), right orbitofrontal (ROF), left subtemporal (LST) and right subtemporal cortex (RST). Depth electrodes are placed in the left

temporal depth (LTD) and right temporal depth (RTD) to record hippocampal EEG activity. (b) Arrangement of electrodes for recording scalp-EEG according to international 10-20 system. 41

4.2 Performance (ROC) of seizure detection algorithm for different combination of thresholds Th_1 and Th_2 (in blue). The green dot marks the best performance. The black dot marks the performance for the threshold selected in our algorithm. The magenta and red dots correspond to cases of worst performance, producing respectively 5% sensitivity and 0 false positives per hour and 95% sensitivity with 1 false positive every 2 hours 45

4.3 60sec of EEG with a subclinical seizure missed by our detection algorithm (Patient-3) 46

Chapter 1

INTRODUCTION

1.1 Overview

The word ‘Epilepsy’ is derived from the ancient Greek word ‘Epilepsia’. The condition was first registered in the East in a Babylonian treatise that was discovered in southern Turkey. In ancient times, epilepsy was considered to be sacred as people believed that it was a form of attack by demons and curse by the gods. This misconception resulted in the discrimination of epileptic patients forcing them to stay in darkness. Hippocrates once remarked that the day epilepsy is understood, it would cease to be considered divine. Today, with the discovery of EEG (Electroencephalography – recording of bioelectrical activity in the brain) and advancements in neuroscience, epilepsy is better understood as a neurological disorder characterized by epileptic seizures that result from abnormal neuronal activity in the brain.

Epilepsy is one of the most common neurological disorders that affect a significant percentage of the world’s population. Approximately one in every 100 persons experiences an epilepsy-related event (epileptic seizure) at some time in their life. Epileptic seizures are often violent disturbances of the normal brain functionality. These seizures are due to the sudden development of highly synchronous abnormal paroxysmal cerebral electrical activity in the brain and can be fairly recurrent in chronic epilepsy. The clinical manifestations of an epileptic seizure include behavioral changes, involuntary motor functions like flexing of arms and legs, eyes rolling towards the back of the head, teeth clenching, facial

twitches or shaking of one or both sides of the body. These clinical symptoms, along with EEG recordings, are used by physicians to detect and evaluate epileptic seizures.

Epilepsy can occur at any age, equally in both sexes, but is most frequently encountered in the very young and the elderly population. Causes for epilepsy include genetic abnormalities, developmental anomalies, febrile convulsions, central nervous system infections, hypoxia, ischemia and tumors. Although patients with epilepsy can lead a normal life, they are usually advised not to participate in any activity that an occurring seizure can put their life in danger (e.g. driving a car). A comprehensive study on the impact of epilepsy and its treatment on patients with epilepsy were carried out using clinical and demographic information and self- completed questionnaires. Data collected from over 5000 patients showed over a third of total patients have frequent seizures with a fifth reporting that their seizures were not well controlled by antiepileptic medication (Baker, Jacoby, Buck, Stalgis, & Monnet, 1997).

Epilepsy can be usually controlled (but not necessarily cured) using available anti-epileptic drugs (AEDs). Epilepsy can lead even to death of the patient due to lack of effective treatment and medication. An estimated 30% of epileptic patients develop medically intractable epilepsy where no seizure control can be achieved with any of the available AED medications. An estimated 42,000 epileptic patients die from Status Epilepticus every year in the United States alone, a condition where seizures occur continuously and the patient can typically recover only with extreme external intervention.

1.2 Electroencephalography

The electroencephalogram (EEG) signal contains information about the electrical activity of the brain and is recorded either from the surface of the head (scalp EEG) or directly from the brain (intracranial EEG). EEG is to date universally accepted as the most reliable clinical tool for understanding epilepsy. Billions of neurons are electrically charged pump ions across their membranes, and create a potential difference that EEG measures over time. EEG measures these voltage fluctuations as differences in voltage between any two recording sites in the brain. It is important for an electroencephalographer to understand that the EEG signal from neuronal population in the brain is greatly modified by the time it reaches a recording electrode. Every electrode will record an average of electrical activity around it along with voltage fluctuations from distant parts of the brain.

Scalp EEG, being a non-invasive recording technique, is plagued by recording and movement artifacts. These artifacts are the potentials generated by sources other than the brain. Physiological artifacts arise from body activities which include head movement, eye blinking, tongue movement, while environmental artifacts originate from power line interferences, electrode movement etc. Because of such noise, and the fact that deeper brain activity cannot be recorded accurately by scalp EEG, an invasive technique where signals are recorded directly from the human cortex using subdural grids or electrodes placed directly on the surface of the cortex is preferred. This recording arrangement is known as Electrocorticography (ECoG). Other specific areas in the brain can be effectively targeted (Intracranial EEG (iEEG)) by using this

approach, thereby improving the information content of the signal. In addition, as these recording electrodes are placed inside the brain, where there is little or no interference from outside sources, the occurrence of artifacts is greatly reduced.

The discovery of EEG by Richard Caton contributed to a better understanding of the electrical activity of the brain. This led Hans Berger to first record human EEG (Brazier, 1961). Using a string galvanometer he was successful in recording alpha rhythms (EEG activity in the frequency range of 8 to 12 Hz). By the year 1960, the usage of clinical and experimental EEG had started to become an important tool in medical institutions and major hospitals to explore mental and psychological processes in the brain. The advancement of computers soon made people believe that EEG interpretation could be completely automated in near future.

Continuous EEG recording has been a boon for all those working in the area of epilepsy research. The main aim of long-term EEG monitoring is to record typical seizures as it helps physicians better diagnose and treat patients and also localize the epileptogenic focus (the region of the brain where seizure originates from). Nowadays, clinical EEG is combined with video monitoring to also record behavioral activities of epileptic patients and produces huge amounts of data. Epileptic activity in the brain corresponds to abnormalities in the EEG recording that allow clinicians and researchers to detect seizures. The motivation behind our research has been the development of an automated seizure detection algorithm to assist physicians in such a laborious, time consuming and expensive task. This

task is costly as a large amount of time is spent on visual marking of epileptic seizures.

To effectively address the seizure detection problem it is important to understand and study normal EEG recordings. An EEG recording, devoid of abnormal patterns associated with a neurological disease, is termed normal EEG. A wide variety of normal EEG patterns can be seen in different individuals in different age groups. Therefore, an electroencephalographer should be able to distinguish and take into consideration all these features of normal EEG at different ages. The most commonly used EEG features are morphology, frequency, amplitude and phase of the EEG signal. It should also be noted that EEG from an epileptic patient should be considered abnormal even if it contains normal EEG components. Normal EEG activity is described in terms of rhythmic activity in specific frequency bands. The classification of EEG signal based on activity in specific frequency bands is listed below:

- Delta rhythm

EEG rhythmic activity below 4 Hz is categorized as delta rhythm. It is most prominent frontally in adults and posteriorly in children. It consists of high amplitude waves found during sleep and while performing tasks requiring continuous attention.

- Theta rhythm

EEG activity in the frequency range 4-8 Hz is categorized as theta rhythm found in young children during sleep. This frequency range of EEG activity has been associated with reports of relaxed, meditative, and creative states.

- Alpha rhythm

EEG activity in the frequency range 8-13 Hz is categorized as alpha rhythm. It consists of regular waveforms with sharp peaks which are prominent in posterior regions of the head while resting. This was the first recorded electrical activity of the brain (recorded by Hans Berger); hence named as ‘alpha rhythm’.

- Beta rhythm

EEG activity in the frequency range 13-30 Hz is categorized as beta rhythm. It has symmetrical distribution on both sides of brain and is most evident frontally. Low amplitude beta with multiple and varying frequencies is often associated with active, busy or anxious thinking and active concentration.

The EEG signal is considered to be abnormal if it contains any epileptiform activity, slow waves and abnormalities of amplitude or certain patterns resembling that of normal activity but deviating from it with respect to certain features like frequency (Fisch, 2003). In a broad classification, epochs of EEG with seizure activity are called ictal EEG, while the rest of EEG is called inter-ictal EEG.

1.3 Classification of Epileptic Seizures

An epileptic seizure, as defined by the International League Against Epilepsy (ILAE) is “a transient occurrence of signs and/or symptoms due to abnormal excessive or synchronous neuronal activity in the brain” (Fisher et al., 2005). The main features used for classification of epileptic seizures are their clinical manifestations and changes in EEG recordings. The most widely accepted

classification of epileptic seizures is defined by the Commission on Classification and Terminology of ILAE. Video and EEG recordings are together used to classify seizures. Based on video monitoring for clinical manifestations, the epileptic seizures can be classified into two main categories:

- Clinical seizures

  These are epileptic seizures which show clinical manifestations as reported by the patient or an observer. These are behavioral events characterized by involuntary movements like flexing of arms and legs, eyes rolling towards back of the head, teeth clenching, facial twitches or shaking.

- Sub-clinical seizures

  These are seizures with no clinical manifestations, but with recorded abnormalities in the EEG. These electrographic events are usually of shorter duration and remain more localized in the brain when compared to clinical seizures.

A second type of classification of seizures, based on the extent of the brain that is affected by a seizure is more general and exhibit 2 major categories:

- Generalized seizures

  These seizures typically affect both hemispheres of the brain (large areas of the cortex or subcortical structures). Such seizures do not have a recognizable focus at onset and usually cause loss of consciousness.

- Partial seizures

  This is the most common type of seizures in children and the electrographic changes are limited to one hemisphere of brain. They are further classified as *Simple Partial Seizures* if there is no impairment in the consciousness of the patient and if they are electrographically limited to a small region of one hemisphere or, as *Complex Partial Seizures* if the patients lose consciousness. In Fig. 1.1 and Fig. 1.2 we show two typical examples of a complex partial clinical seizure and a simple partial sub-clinical seizure respectively. The subclinical seizure is comparatively of lesser duration and spatial extent.

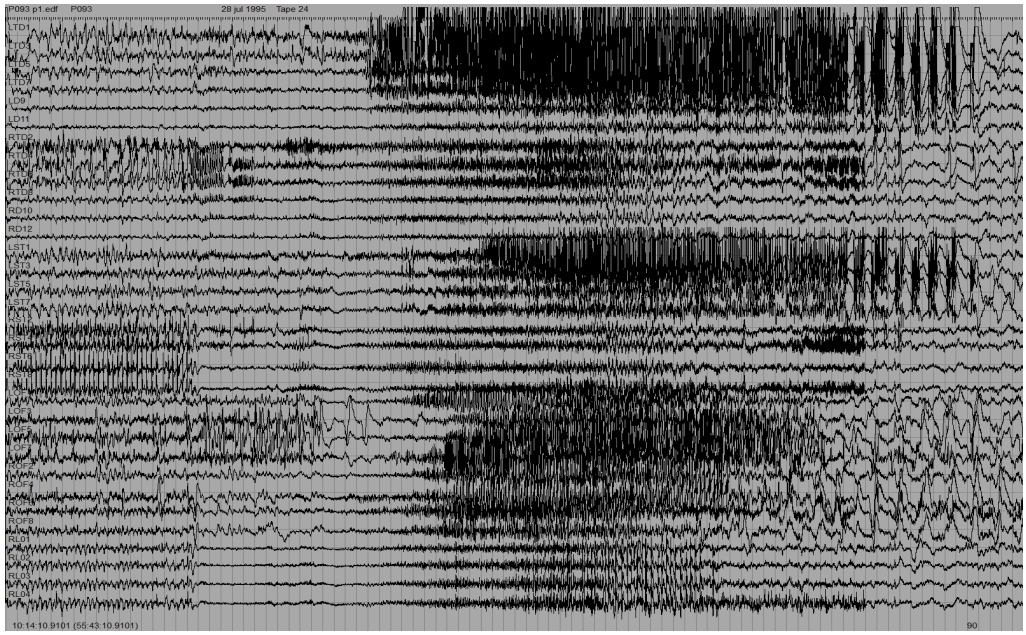

Figure 1.1: 90sec of intracranial EEG with a secondarily generalized complex partial seizure clinical seizure. Seizure onset is the right hippocampus.

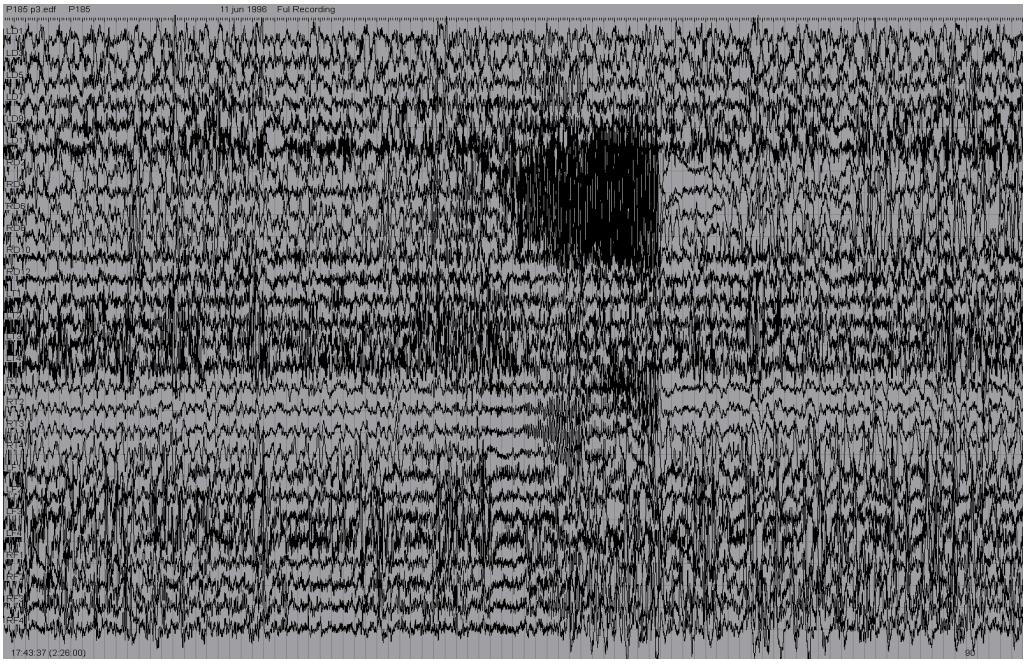

Figure 1.2: 90sec of EEG with a simple partial sub-clinical seizure.

1.4 Brain Dynamics

It is important to understand the complexity of the human brain in the search of causes for epilepsy. Human brain can be seen as a highly complex, nonlinear system with changes in its dynamics that can be used to distinguish an epileptic from a normal brain. Comprehensive studies in EEG-Brain dynamics have been carried out in the past (Başar, 1980). Complex nonlinear systems can be studied either through mathematical modeling or time series analysis. Time series analysis has advantages over mathematical models as it is difficult, if not impossible, in the case of the human brain to find analytical solutions to nonlinear equations in closed form.

The early belief that epileptic seizures could not be anticipated was due to the assumption that seizures were abrupt transitions that occurred randomly. The ability to predict epileptic seizures well in advance of their occurrence may lead to better treatments of epilepsy. For example, this can be achieved by using the EEG signals to monitor the dynamical changes of the brain over time and intervene therapeutically at the right time. Seizures can be considered as manifestations of dynamical changes of a chaotic nonlinear system that can be captured by measures of chaos, such as the Lyapunov exponents (Benettin, Galgani, Giorgilli, & Strelcyn, 1980; Shimada & Nagashima, 1979). The hypothesis that the brain progresses into and out of different states of chaos was formulated in the past (Iasemidis et al., 2003). A group led by Iasemidis, Sackellares and Williams, was the first to report application of nonlinear dynamics to clinical epilepsy (L. Iasemidis, Zaveri, Sackellares, Williams, &

Hood, 1988). It was also the first time NIH (National Institute of Health) supported a clinical investigation into the application of nonlinear dynamics theory on epileptic seizures. This hypothesis changed some long-held beliefs about predictability of epileptic seizures. The transition from normal states to epileptic seizures was explained as a deterministic process (L. D. Iasemidis, Olson, Savit, & Sackellares, 1994; Olson, Iasemidis, & Sackellares, 1989). Nonlinear dynamical analysis of EEG recorded with subdural electrodes showed the existence of long-term preictal periods (order of minutes) and increased the prospects of seizure prediction algorithms by monitoring the evolution of short-term Lyapunov exponents (STL_{max}) (L. D. Iasemidis, Chris Sackellares, Zaveri, & Williams, 1990; L. D. Iasemidis & Sackellares, 1991; L. Iasemidis et al., 1997; Sackellares, Iasemidis, Shiau, Gilmore, & Roper, 2000). The estimated Lyapunov exponents in the above approaches are used to measure the information flow (bits/sec) along local eigenvectors as the brain moves within its state space. Application of the same technique to epileptogenic focus localization was also reported (M. C. Casdagli et al., 1997; M. Casdagli et al., 1996).

1.5 Research Objectives

The main aim of this research is to provide an efficacious alternative to the visual detection of seizures from long-term (days to weeks) continuous EEG recordings by developing an automated, training-free, patient-independent, data-adaptive robust algorithm using measures from linear and nonlinear dynamics. Two new measures, Adaptive Teager Energy (ATE) and Adaptive Short-Term maximum

Lyapunov exponent ($ASTL_{max}$) are introduced in this thesis to capture changes in the energy and nonlinear dynamics of the EEG signal respectively. Epochs of ictal activity (seizure) typically possess higher energy when compared to epochs of inter-ictal (non-seizure) events. This difference in energy can be captured using ATE, but is not specific only seizures. However, dynamics corresponding to ictal epochs may be different from those of non-ictal epochs and this difference can be captured using the maximum Lyapunov exponent. The innovation is estimate the Short-term Lyapunov exponent as data-adaptive by selecting the parameter of time lag τ in the reconstruction of the state space of the brain over time. The sample autocorrelation function was used to estimate the time lag for every 30sec EEG segment. The data-adaptive Teager energy was also estimated using the same time lag.

1.6 Thesis Organization

This thesis is organized as follows. Chapter 2 outlines a brief description of dynamical systems and chaos theory, Lyapunov exponents, Teager energy and autocorrelation function. Application of all these measures to EEG is presented. The estimation procedure of our proposed measures, $ASTL_{max}$ and ATE, in the seizure detection algorithm is explained in this chapter. Chapter 3 describes the steps involved in the automatic selection of the optimal electrodes to be followed over time. An example of application of the algorithm to a single electrode EEG recording with one seizure is presented. Results of the performance of the

algorithm in all patients analyzed, including possible variations of it are presented in chapter 4. The overall result of this research is summarized in chapter 5.

Chapter 2

METHODS AND TOOLS

2.1 Dynamical Systems and Chaos

Dynamics is the study of changes of the states of a system as it evolves in time. Chaos theory studies the behavior of nonlinear dynamical systems, like the brain, that are highly sensitive to initial conditions. Any perturbation to the initial conditions of such systems yields widely diverging dynamics. This behavior is known as deterministic chaos. Convincing evidence for existence of deterministic chaos has been provided from a variety of research experiments (Roux, Simoyi, & Swinney, 1983; Swinney, 1983). Differential equations have been used to model physical systems to determine how they behave temporally under different experimental conditions and so try to predict their future states. Modeling a physical system using differential equations is essentially impossible when the order and degree of the modeled systems are very high. Nonlinear systems with closed form analytical solutions typically settle in a steady state or in a periodic motion. In 1975, a new kind of motion was observed which was erratic. This type of motion was termed chaos, and the theory developed to explain such systems as chaos theory.

Many natural systems showing chaotic behavior have been comprehensively studied (Hastings & Powell, 1991; Schaffer, 1985), the most famous one being the weather. The initial study on chaos theory was pursued by a meteorologist, Edward Lorenz, while working on weather prediction models. He was running his experiments on a computer with a set of differential equations to

model the weather. When he started the same experiment with a different set of initial conditions, he found that rounding-off errors in initial conditions had a large influence on the subsequent dynamics of the model equations.

A system is said to be in an unstable steady state if small perturbations make the system evolve away from the steady state. For example a cone resting on its apex can be balanced at just one particular point. But if the cone is perturbed it falls to the ground which is its stable state. A system may experience more complicated steady states, in the sense that there are many regions in the state space the system may eventually rest to or stabilize in. Even though nearby points in the state space of a chaotic system move away from each other, a steady chaotic state can dynamically be defined as stable if the system always moves (according to a deterministic probability distribution) within it and never escapes from it under a small bounded perturbation (chaotic attractor).

A detailed description of such systems was first described mathematically by Lorenz in his seminal paper in 1963. He presented a system of 3 coupled differential equations which behave chaotically. This led him to his now famous speculation that a butterfly flapping wings in Brazil (which is a small change in the initial conditions in the atmosphere) might cause a tornado in Texas. This dependence of the evolution of a system on its initial conditions makes chaotic motion a complex phenomenon. In this sense, it is intuitive to expect that systems in nature are complex, and the larger the number of system's state variables, the more complex the system is.

It is important to understand the properties of chaotic systems, some of which are:

i. *Determinism:* Even though chaotic systems exhibit random behavior, they are classified as deterministic systems. This is because if the initial conditions are known precisely, future behavior of the system can be predicted. However, initial conditions are never known for a real system.

ii. *Nonlinearity:* Nonlinearity is a necessary condition for a system to exhibit chaos. A perfectly linear system can never exhibit chaos.

iii. *Sensitivity to initial conditions:* This is the most important characteristic of chaotic systems. Chaotic systems for any two different initial conditions (however close) always diverge exponentially as they evolve in time. Hence, a small change in the initial conditions takes the system in a completely different trajectory.

iv. *Boundedness:* If the divergent orbits go to infinity, the system is considered not to be chaotic as the system is unbounded and cannot produce steady states.

2.1.1 Lorenz Attractor

The Lorenz attractor is the steady state of a nonlinear chaotic system of three coupled nonlinear ordinary differential equations (Tucker, 1999). These equations were derived by Lorenz in 1963 and represent a simplified model of thermal convection in the lower atmosphere. Lorenz showed that this relatively simple-looking set of equations (shown in Eq. 2.1) could have highly erratic

dynamics for a range of defined parameters, under which the dynamics are chaotic. These unique equations are:

$$\dot{x} = \sigma(y - x) \tag{2.1}$$

$$\dot{y} = rx - y - xz$$

$$\dot{z} = xy - bz$$

where x, y, z are the state variables and σ, r and b>0 are dimensionless parameters. A sample trajectory in the 2 and 3 dimensional state space generated from these set of equations is shown in figure 2.1.

Upon close inspection of the plots shown in Fig. 2.1, the trajectories depicted therein never intersect each another. For any small perturbation of initial conditions, the state-space trajectory will never follow the same path. Furthermore, if one were to plot the trajectories of the solution for one set of initial conditions and then for another set of initial conditions (infinitesimally close to the first), the two trajectories would diverge from one another exponentially. This means that not only does a small perturbation to initial condition result in a trajectory that will never intersect with that of the original system but it results in a completely different trajectory.

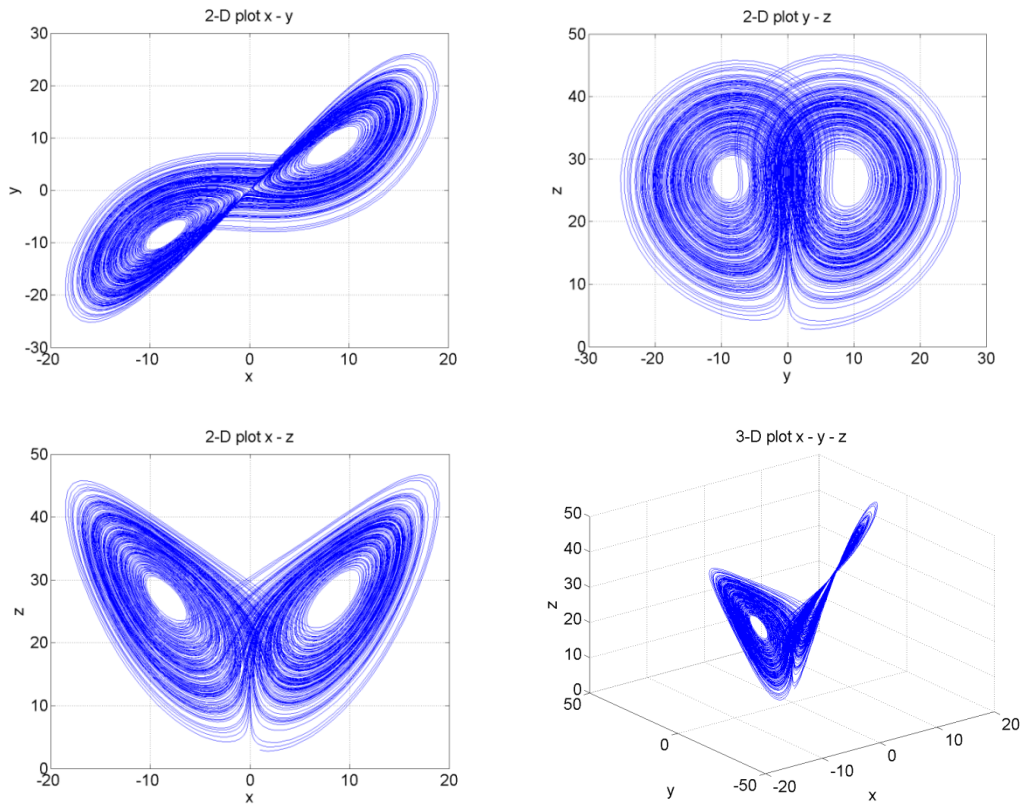

Figure 2.1: Lorenz system: Trajectories in the state space with initial conditions x(0)=1, y(0)=2 and z(0)=3 and parameters σ=10, b=8/3, r=28 and N=20400.

2.2 State Space Representation and State Space Reconstruction

For a discrete dynamical system the state space (or phase space) is a vector space in which all possible states of a system are represented with a unique vector (set of points). The rank of this space gives the necessary number of degrees of freedom or variables the system may have.

For a mathematically modeled system, its system equations can be used to create the state space. However, for real-world chaotic dynamical systems, the system equations are unknown and hence we have to employ methods of attractor

reconstruction to obtain the state space. We will follow the approach developed by Takens (Takens, 1981), which is based on the method of the delay coordinates for reconstruction of the state space (embedding) of an unknown system. The embedding method has been proven useful, particularly for time series generated from low-dimensional, deterministic dynamical systems. This approach of state space reconstruction has found its applications in several fields in engineering and has been a favorite approach in the analysis of epileptic EEG signals for seizure prediction (L. D. Iasemidis et al., 2003) and epileptogenic focus localization (L. D. Iasemidis et al., 1990; Sabesan et al., 2009).

Takens' delay embedding theorem states the conditions under which a chaotic dynamical system can be reconstructed from its observations and is explained as follows:

For a given measured time series $x_i(t)$, the time-delay vectors (embedding vectors) $X_i(n)$ are given by

$$X_i(n) = \{x_i(n), x_i(n+\tau), \dots, x_i(n+(m-1)\tau)\} \qquad (2.2)$$

where 'm' is the embedding dimension which should be sufficiently large for a perfect state space reconstruction and τ is the time-delay (or embedding lag). These parameters have to be carefully selected in order to facilitate a good state space reconstruction. An embedding dimension of m=7 for epileptic seizures has been reported by Iasemidis et al (Olson, Iasemidis, & Sackellares, 1989) and is used in our research too. According to Takens, in order to properly embed a signal in the state space, the embedding dimension should at least be equal to $2D + 1$, where D is called as the Box Counting Dimension or Minkowski-Bouligand

dimension (Dubuc, Quiniou, Roques-Carmes, Tricot, & Zucker, 1989; Pašić, 2003). One of the measures used to estimate D is the state space correlation dimension (Liebovitch & Toth, 1989). The brain, being a nonstationary system, is not expected to be in a steady state in the strict dynamical sense at any location. The activity at brain sites is constantly moving through steady states, which are functions of certain parameter values at a given time. According to bifurcation theory, when these parameters change slowly over time (e.g., when the system is close to a bifurcation point), dynamics slow down and conditions of stationarity are better satisfied. In the ictal state (Haken, 1996), temporally ordered and spatially synchronized oscillations in the EEG usually persist for a relatively long period of time (in the range of minutes).

Dividing the ictal EEG into short segments ranging from 10.24 sec to 50 sec in duration and estimating ν from ictal EEG has produced values between 2 and 3 (L. Iasemidis, Principe, & Sackellares, 2000), implying the existence of a low-dimensional manifold in the ictal state. Therefore, an embedding dimension m of at least 7 can be used to properly reconstruct the attractor of the ictal state. The embedding dimension for inter-ictal (between seizures) period is expected to be higher than that of the ictal state, but a constant embedding dimension of m=7 will be used in this thesis to reconstruct all relevant state spaces from both ictal and inter-ictal period, so that comparison of measures from the two periods makes physical sense. The advantage of this approach is that any irrelevant information in dimensions higher than 7 would not affect our results. The disadvantage is that relevant information in higher dimensions than m=7 is missed.

The time-delay τ can be estimated from the decay time of the autocorrelation function. The purpose of time delay τ is to make the components of the vectors in the embedding sufficiently independent. A low value of the delay time results to adjacent components be correlated and hence they cannot be considered as independent variables. On the other hand, a high value of delay may make the adjacent components uncorrelated (almost independent) and cannot be considered as part of one system that supposedly generated them. Methods used to estimate an optimum time delay are the first minimum of the mutual information, the 1/e of autocorrelation and the first zero of the autocorrelation (Abarbanel, 1996).

2.3 Lyapunov Exponents

A positive Lyapunov exponent is a signature of chaos. A chaotic system has at least a positive Lyapunov exponent. This is because of the exponentially growth over time of distances of initially nearby states. The Lyapunov exponent measures the rate of a trajectory's divergence (or convergence) over time. A positive Lyapunov exponent indicates orbital divergence and hence chaos in the system. A negative Lyapunov exponent indicates orbital convergence and hence a dissipative system. Wolf et al. described the first practical algorithm for estimating the largest Lyapunov exponent from real data by following the divergence/convergence rate of nearby trajectories (Wolf, Swift, Swinney, & Vastano, 1985).

The Lyapunov exponents measure the information flow in bits/sec along local eigenvectors in the state space as the system moves through such attractors. An improved method for calculating this dynamical measure from experimental EEG data has been published by Iasemidis & Sackellares (L. Iasemidis, Principe, & Sackellares, 2000). This method to estimates an approximation of $L_{\max}$ from nonstationary data, called STL (Short-term Lyapunov), developed via a modification of the Wolf's algorithm used to estimate $L_{\max}$ from stationary data. The procedure is depicted in Fig. 2.2 and is given by the formula

$$STL_{\max k} = \frac{1}{\Delta\, t} \log_2 \frac{\left|X(t_{ik} + \Delta\, t) - X(t_{jk} + \Delta\, t)\right|}{\left|X(t_{ik}) - X(t_{jk})\right|} \tag{2.3}$$

The estimation of the largest Lyapunov exponent ($L_{\max}$) in a chaotic system has been shown to be more reliable and reproducible than the estimation of the remaining exponents, especially when the correlation dimension is unknown and changes over time, as is in the case of high-dimensional and nonstationary data (e.g., interictal EEG).

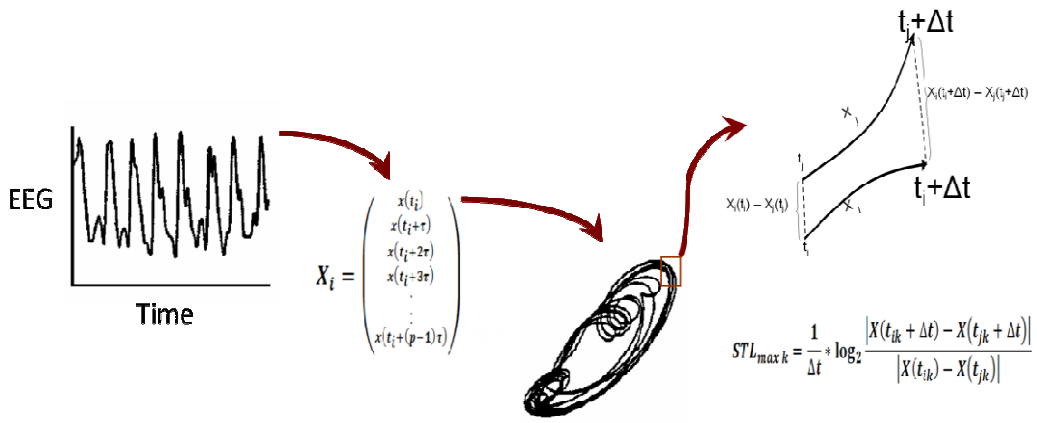

Figure 2.2: State space reconstruction of EEG data by the method of delays

2.4 Teager Energy (TE)

Teager energy operators (Kaiser, 1993) are defined in both the continuous and discrete domains and are very useful tools for detecting single components of signals from an energy point of view. This energy function is a local property of the signal depending on the signal amplitude and its first two derivatives. It is a popular algorithm having wide applications in the field of signal processing due to its simplicity in implementation. In continuous time domain, TE is defined by the formula,

where is the first derivative of *x*, and is the second derivative of *x*.

In discrete time domain, TE is defined by the formula,

We know that ictal EEG is characterized by high frequency and high amplitude oscillations and hence possesses higher signal energy when compared to inter-ictal EEG with low frequency and low amplitude oscillations. Thus, TE can in principle differentiate between ictal and inter-ictal EEG segments.

While the performance of TE was found to be good for high SNR, for low SNR its performance is markedly reduced. An improvement of the traditional TE is called multi-resolution TE and was proposed for detection of action potentials, and outperformed the traditional TE (Choi & Kim, 2002). The new measure was called k-TEO and is given by

$$\Psi_k(x[n]) = x_n^2 - x_{n-k}x_{n+k} \tag{2.6}$$

The parameter *k* is optimized to give the best performance. In a real case scenario, this optimal value for *k* varies over time, and hence having a single value for *k* reduces the algorithm's performance, which is a major drawback.

2.5 Autocorrelation Function

Autocorrelation is a statistical measure used to describe the correlation between observations (how closely the observations are related) of a dataset for different time lags τ. It can be seen as a measure to detect the presence of any related periodic patterns in a dataset. In statistics, is given by the formula,

$$R(\tau) = \frac{E[(X_t - \mu)(X_{t+\tau} - \mu)]}{\sigma^2} \tag{2.7}$$

where μ is the mean of all observations with a variance of σ^2 .

The autocorrelation function is estimated by the Sample Autocorrelation. It is a widely used measure to find the embedding lag τ for nonlinear time series analysis. For a process X_t, the sample autocorrelation is given by the formula,

$$\rho(\tau) = \frac{\sum_{n=1}^{N}(x_n - \bar{x})(x_{n+\tau} - \bar{x})}{\sum_{n=1}^{N}(x_n - \bar{x})^2} \tag{2.8}$$

where $\bar{x} = \frac{1}{N}\sum_{i=1}^{N} x_i$, is the sample mean and *N* is the number of observations.

2.6 Ictal vs Inter-ictal EEG

To design an algorithm for seizure detection, it is important to understand the difference between ictal and inter-ictal EEG. Two datasets, one with ictal EEG segments and another with inter-ictal EEG segments from the same patient, were first analyzed from a single electrode resulting in 5 ictal EEG segments and 117 inter-ictal EEG segments (duration of 30sec with 20sec overlap). The frequency band 0-15 Hz of EEG from these two datasets was divided into sub-bands using band-pass filters with bandwidth of 1Hz. Average power spectral density was estimated for each of these bands using Welch periodogram. The lag index corresponding to the point where the value of the autocorrelation function crosses a lower confidence bound was used as an estimate for delay time τ using the formula

$$\tau = \frac{Lag\ Index}{Embedding\ dimension - 1} \tag{2.8}$$

STL_{max} values for these segments where then estimated using their respective delay time τ. The results of this analysis are given in Tables 2.1 and 2.2.

Table 2.1: Analysis of Ictal vs Inter-ictal EEG (30sec with sub-band frequencies)

	Ictal EEG Analysis			**Inter-ictal EEG Analysis**		
Frequency Band (Hz)	**Average PSD (μW/Hz)**	**Tau (mean)**	**STL_{max} (mean) (bits/sec)**	**Average PSD (μW/Hz)**	**Tau (mean)**	**STL_{max} (mean) (bits/sec)**
0-1	0.0304	12.8	2.3384	**0.0569**	**13.5726**	**2.0952**
1-2	0.1293	5.2	4.0093	**0.0442**	**6.1795**	**3.5536**
2-3	0.2198	3.6	4.2445	0.0159	4	3.8563
3-4	**0.2248**	**3**	**3.7923**	0.0098	3	3.7989
4-5	**0.2195**	**2**	**3.9673**	0.0054	2	4.4882
5-6	0.2187	2	3.4582	0.0037	2	3.5942
6-7	0.1046	2	2.7230	0.0030	2	2.9241
7-8	0.0695	1	4.8693	0.0020	1	5.4545
8-9	0.0636	1	5.0614	0.0013	1	4.7323
9-10	0.0558	1	3.6738	0.0009	1	3.9764
10-11	0.0536	1	3.0993	0.0008	1	3.5396
11-12	0.0437	1	3.3560	0.0007	1	3.5040
12-13	0.0450	1	3.0684	0.0006	1	3.1765
13-14	0.0304	1	3.2492	0.0005	1	2.9894
14-15	0.0250	1	2.3577	0.0004	1	2.9181

Table 2.2: Analysis of ictal and inter-ictal EEG (with all frequencies)

	Tau (mean)	**STL_{max} (mean)**
Ictal	2.6	5.9360
Inter-Ictal	8.3162	2.0978

From Table 2.1, we see that the frequency band between 3-5Hz has the highest average power spectral density for epochs of ictal EEG. The corresponding time lags τ are between 2 and 3. On the other hand, for inter-ictal

epochs of EEG, the highest average PSD is in the frequency band 0-2Hz with time lags between 6 and 13. Additionally, the corresponding STL_{max} values for these bands indicate that the inter-ictally more dominant slow activity (1-2Hz) is more ordered (STL_{max} =2-3) than the dominant activity (3-5Hz) in the ictal state (STL_{max} =3-4).

Estimation of STL_{max} and time lag for the same ictal and inter-ictal segments of EEG without sub-band filtering are shown in Table 2.2. The time lag selected for both the interictal and ictal segments corresponds to the time lag obtained from the filtered data at the frequency bands with the highest average PSD. In this sense the use of a data-adaptive lag in the estimation of STL_{max} effectively acts as a filtering process that automatically captures the dominant frequency in the signal. This is especially useful in the case of seizure detection, since there is no uniqueness in the ictal frequency activity that is present in different types of seizures, or even in different seizures from the same subject.

Using these initial observations, we designed an algorithm using adaptive estimation of the involved parameters from the data. In the next section, we present the two measures used in our proposed seizure detection algorithm.

2.7 Adaptive Lyapunov exponents ($ASTL_{max}$)

In traditional STL_{max} estimation, the time lag τ is fixed for EEG analysis optimized for reconstruction of the state space from the ictal period. The idea here was to capture ictal features of the system (brain) as it moves from a normal state (inter-ictal) towards an abnormal state (ictal), and thus facilitate the prediction of

such events. Here, our aim is to detect rather than predict seizures. We have seen from the previous section that there is a clear distinction between ictal and inter-ictal EEG if we use different time delays in the state space reconstruction. Hence a constant value of time delay is not advisable for use in a seizure detection algorithm.

Fig. 2.3 shows that $ASTL_{max}$ values are different for ictal EEG when compared with pre-ictal and post-ictal EEG. Activities in low frequency (0-2 Hz) during pre-ictal and post-ictal periods correspond to lower complexity (low values of $ASTL_{max}$). On the other hand, activities in the high frequency (3-5 Hz) correspond to higher complexity (higher $ASTL_{max}$). This difference in the values of the $ASTL_{max}$, in conjunction with the one in Teager energies (see next section) is used to detect a seizure by our algorithm.

2.8 Adaptive Teager Energy (ATE)

In accordance to the estimation of $ASTL_{max}$ we propose an adaptive time lag τ, derived from sample autocorrelation function, as the lag index k for TE. The rationale for the use of an adaptive TE is the same as in (Choi & Kim, 2002), i.e., to utilize its sensitivity to the frequency content of the signal. Hence, ATE can be defined by the following equation

$$\Psi_k(x[n]) = x_n^2 - x_{n-\tau}x_{n+\tau} \tag{2.9}$$

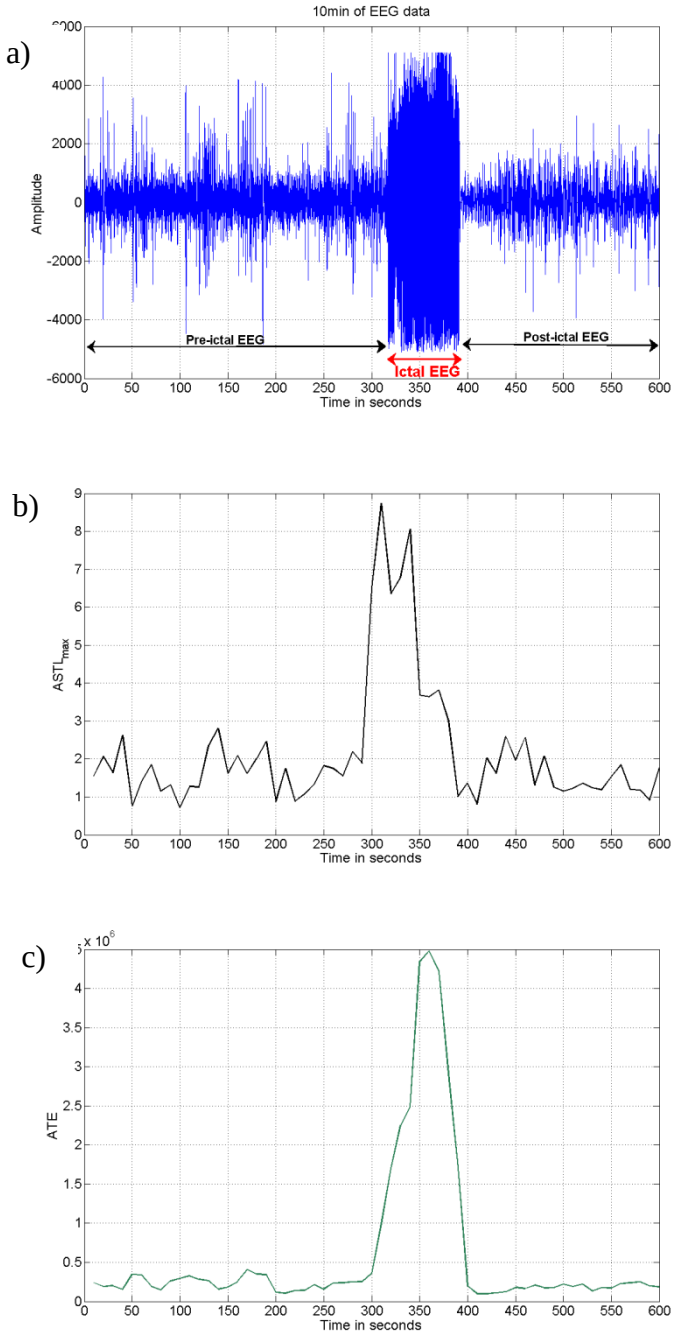

Figure 2.3: Teager Energy for 10minutes of EEG from electrode RD4 in Patient-3 that includes a seizure: (a) Sample EEG with a seizure at 300sec (blue). (b) $ASTL_{max}$ values (black) estimated every 10 sec(c) ATE values (green) estimated every 10 sec.

Chapter 3

SEIZURE DETECTION

3.1 Background

The task of detecting epochs of EEG having seizure-like activity is non-trivial due to several factors, including the differences in seizure morphologies within and across patients, and the presence of movement and other recording artifacts. This has motivated researchers to work towards the development of robust seizure detection algorithms. An initial automated seizure detection algorithm was designed by Gotman (Gotman, 1982), using recorded events like seizure anticipation/experience by the patient or an observer, and spikes detected by an automatic spike recognition program. This experimental setup facilitated the study of correlation between electrographic seizures (epileptic activity recorded in the EEG) and their clinical manifestations. In a similar study, it was estimated that nearly 30% of electrographic seizures are not accompanied by clinical manifestations (Ives & Woods, 1980). These studies showed that a seizure detection algorithm based on electrographic recordings always outperforms the push-button approach which uses perception of a seizure by the patient or an observer. The earlier approach by Gotman depended heavily on amplitude changes in the EEG recording and was found that even with the assistance of an artifact removal system to cancel false positives the algorithm reached at most a sensitivity of 70-80%. The algorithm was later updated with modifications and after extensive evaluation it is now integrated into several commercial medical devices for clinical use (Gotman, 1990). Despite the modifications and

improvements the algorithm still suffers performance-wise, with the major drawback being the large number of false positives (1-3 per hour).

Automated seizure detection based on artificial neural networks involves a training procedure that improves the algorithm's performance. The training involves samples of seizure and non-seizure segments, thereby making the algorithm learn to discriminate between these segments in future (testing) EEG data. The detection performance of these algorithms relies on the features extracted from EEG during the training phase. Webber et al. (Webber, Lesser, Richardson, & Wilson, 1996) have reported on the use of amplitude, slope, curvature, rhythmicity, and frequency components of EEG in 2sec epochs that improves the specificity to 1 false positive/hr. Gabor et al. (Gabor, Leach, & Dowla, 1996) used an unsupervised training approach in conjunction with a matched filter constructed by wavelet transform using 8-channel subsets of 18 channel scalp EEG recordings. Their algorithm achieved 90% sensitivity with a considerable reduction in false positives rate to less than 1 per hour. A seizure detection algorithm primarily aimed at intracranial EEG developed by Osorio et al. (Osorio, Frei, & Wilkinson, 1998) claimed an ideal sensitivity of 100% with no false detections utilizing advanced digital signal processing techniques like in time-frequency localization, image processing and identification of time-varying stochastic systems. It should be noted though, that their algorithm was not evaluated on continuous EEG. A wavelet-based approach for seizure detection in intracranial EEG was presented by Khan et al. (Khan & Gotman, 2003) claiming a reduction in false detections to 0.3 per hour. Usually, the length of training data

is more than the length of testing data, which in itself should be considered as a disadvantage for the development of a seizure detection algorithm. Additionally, the huge variability of seizures across patients makes it harder to have a trained network on a set of one patient's EEG recordings and test it on another patient.

Single electrode time-frequency analysis using matching pursuit algorithm was applied qualitatively for detection of seizures originating from the mesial temporal lobe (Franaszczuk, Bergey, Durka, & Eisenberg, 1998). Significant parts of the ictal period like initiation, rhythmic bursting activity, organized rhythmic bursting activity and intermittent bursting activity were identified in this study. Recently, attempts have been made towards applications of nonlinear techniques for seizure detection. The findings in (Päivinen et al., 2005) suggest that best results could be achieved by using a combination of linear and nonlinear measures as features for seizure detection. A novel wavelet-chaos neural network method for EEG segment classification into healthy, ictal, and inter-ictal EEGs using correlation dimension and largest Lyapunov exponent was introduced by Adeli et al. (Adeli, Ghosh-Dastidar, & Dadmehr, 2007). It was shown in this study that the largest Lyapunov exponent can be effectively used to classify ictal and inter-ictal EEG.

Approaches based on artificial neural networks have improved the seizure detection performance at the cost of algorithm's training. The attempts made towards development of algorithms for classification of segments of EEG can be used to assist in the development of algorithms for online seizure detection. Algorithms based on user-defined thresholds prevent the use of such algorithms

across patients without any intervention of a trained person. We focused our research towards development of a seizure detection algorithm eliminating the need for algorithm's training or user-defined thresholds. We intended to develop an algorithm which is patient-independent and data-adaptive eliminating the need for any changes in the algorithm when applying it across patients. Although our final aim is to develop a real-time seizure-onset detection algorithm, we worked towards development of an online seizure detection algorithm during this MS research.

3.2 Seizure Detection Algorithm

Our automated seizure detection algorithm with data-adaptive threshold and capability of selecting the "optimum electrode" over time for seizure detection is presented below.

- Preprocessing of EEG

  The sampling frequency of the multichannel analog EEG across patients was typically 200 Hz or down-sampled to 200 Hz. The digital EEG recording was filtered to remove noise and artifacts in frequency bands outside 0.1-30 Hz. This digitally filtered EEG signal was then segmented into overlapping 30sec epochs (20sec overlap per consecutive epochs).

- Embedding dimension m for reconstruction of the state space per EEG epoch and electrode site

  We selected $m = 7$ for reconstruction of state space as per the findings reported by Iasemidis et al (L. Iasemidis, Principe, & Sackellares, 2000).

- Time lag τ for reconstruction of the state space per EEG epoch and electrode site

  For every 30sec EEG segment the time lag τ at which the sample autocorrelation of this segment first reduces to zero is estimated.

- Adaptive Estimation of the Maximum Lyapunov exponent

  The Adaptive Short-Term maximum Lyapunov exponent ($ASTL_{max}$) is then estimated from the state space reconstructed as above for each EEG epoch according to Iasemidis et. al algorithm (L. Iasemidis, Principe, & Sackellares, 2000).

- Adaptive Teager Energy (ATE)

  The data Adaptive Teager Energy is calculated using the previously estimated time lag τ for each EEG epoch.

- Seizure detection algorithm

  The $ASTL_{max}$ and ATE measures are used in cascade for seizure detection. The following steps are employed towards this goal:

i. 360 values of $ASTL_{max}$ and ATE per electrode (corresponding to 1 hour of EEG) are fed into the electrode selector routine. The parameter 360 was selected so that we have enough data for a statistically sound selection of an electrode in step (ii) and detection of outliers in step (iii) below.

ii. The electrode selector selects one "optimum electrode" per EEG epoch based on the range of the $ASTL_{max}$ values. The electrode that exhibits the maximum range in $ASTL_{max}$ values is selected for further analysis.

iii. From the $ASTL_{max}$ values of the electrode selected in (ii) above, a statistical threshold is calculated as:

$$Th_1 = mean(ASTL_{max}) + 5 * standard\ deviation(ASTL_{max}) \quad (3.3)$$

which implies statistical significance of α=0.00001.

$ASTL_{max}$ values above Th_1 (outliers) are then identified and stored as possible segments S_i that contain seizures. The EEG data of the identified segments S_i are subsequently given as input to the next step (iv) for the algorithm to further refine the detection of possible seizures using ATE.

iv. The ATE values for the 1 hour EEG segment under consideration, and only for the electrode selected in step (iii) above, are employed to define a second threshold Th_2 for outliers such that

$$Th_2 = mean(ATE) + 3 * standard\ deviation(ATE) \quad (3.4)$$

with statistical significance of α=0.001.

We should note that the condition of having at least 2 ATE values to stay above the threshold Th_2 to generate a seizure warning corresponds to a

statistical significance equal to α^2=0.001*0.001=0.00001, the same used in step (ii).

Then for every candidate EEG segment S_i that was identified in step (iii) 21 consecutive TE values that span about 2minutes, that is, its immediate previous ten 10sec segments, the segment itself and its immediate ten subsequent segments are considered. Seizure detection in S_i is declared if at least 2 out of the 21 ATE values are found to be above Th_2. In this case, we conclude that a seizure is included in that 30sec EEG segment S_i. The values 21 and 2 we assigned to the relevant parameters of the algorithm in this step were selected so that

a) Seizures of 2 minutes maximum duration (typical for focal temporal lobe clinical seizures we analyzed) are captured.

b) Seizures of duration as short as 40sec (typical for subclinical seizures in patients we analyzed) are captured.

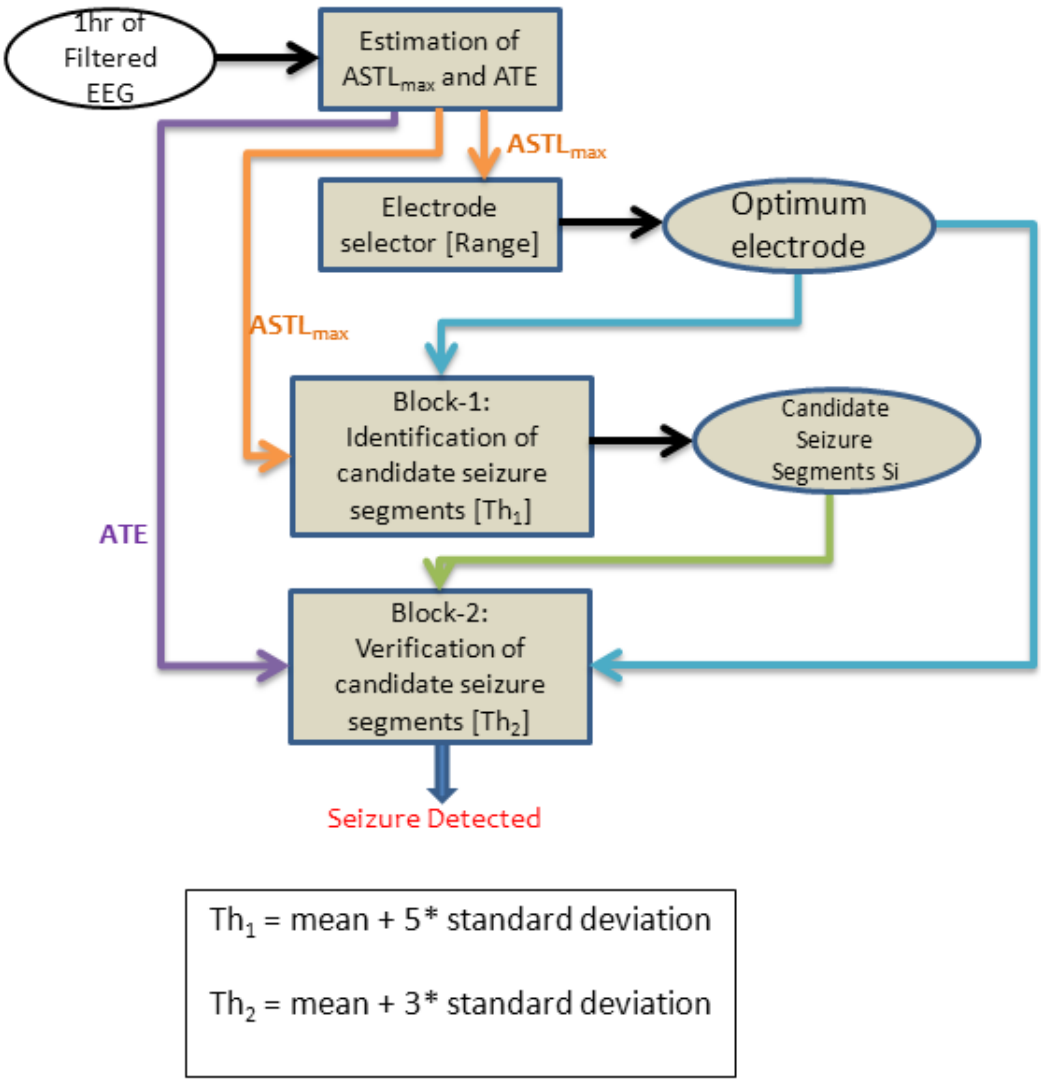

Figure 3.1: Flowchart of Seizure Detection Algorithm

3.3 Example of Application of our Seizure Detection Algorithm

The workings of our seizure detection algorithm with a step-by-step flow analysis will be explained in this section. Our algorithm can be perceived as a 2-block procedure, with one block detecting all possible segments that include seizures (sensitivity) and the second block verifying them (specificity).

An EEG segment of duration 1 hour containing a seizure was selected from Patient-3. The algorithm's steps for this segment are shown in Fig. 3.2(a)-(d). Initially the $ASTL_{max}$ values for all electrodes are given to the electrode selector routine. For clarity of presentation, $ASTL_{max}$ values from only four electrodes are shown in Fig. 3.2(a). The selector routine picks electrode Electrode2 as the optimum electrode for seizure detection. Fig 3.2(b) shows $ASTL_{max}$ values of Electrode2 along with the threshold Th_1. It was verified from visual inspection of the EEG that only the segment corresponding to the first peak (marked in green as true detection) contained seizure activity whereas the other two peaks (marked in red as false detections) did not. The corresponding ATE values for Electrode2 are shown in Fig 3.2(c), where we can see that the two false detections from $ASTL_{max}$ were cancelled since the respective ATE values fall below Th_2.

It should also be noted that ATE in block-2 produced 1 false detection (marked as false detection in red in Fig 3.2(d)). But this had no effect as $ASTL_{max}$ values in block-1 did not generate any warning. The above example was carefully selected to show the working of both measures, $ASTL_{max}$ and ATE in tandem. A more detailed analysis that shows that this setup is optimal is presented in chapter 4.

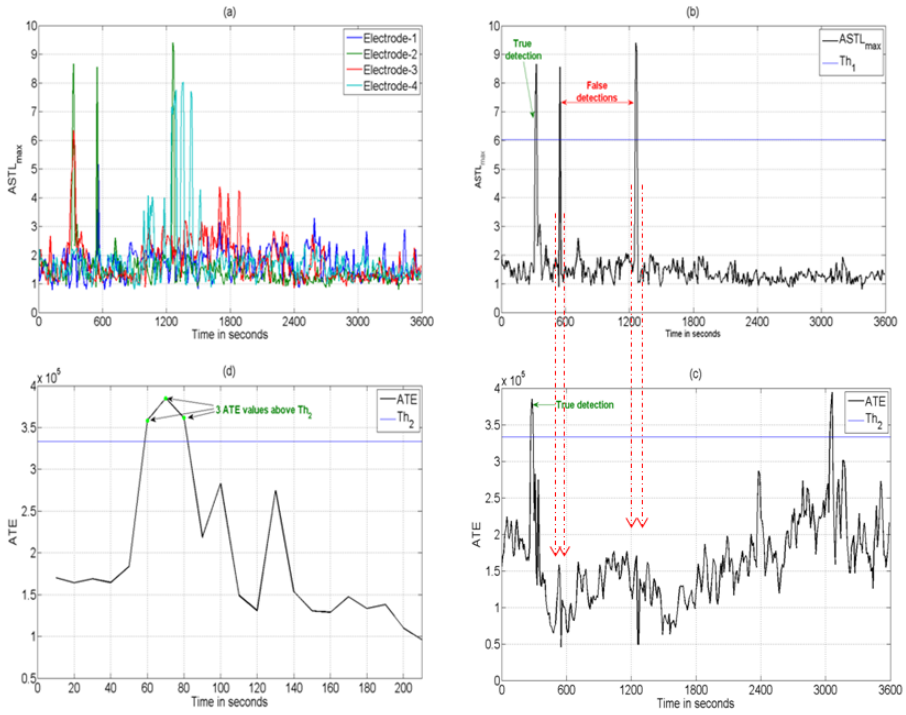

Figure 3.2: Flow of seizure detection algorithm: (a) $ASTL_{max}$ values for 1 hour of EEG recording from 4 electrodes. (b) $ASTL_{max}$ values of selected electrode (Electrode-2) with threshold Th_1. (c) ATE values of Electrode-2 with threshold Th_2. (d) 21 ATE values of Electrode-2 corresponding to peak (marked as True detection in green) in (c). Seizures are announced if outliers occur at the same time in both Figures 3.2(c) and 3.2(d).

Chapter 4

APPLICATION TO SCALP AND INTRACRANIAL EEG

4.1 EEG Data Acquisition

For our study, data from intracranial EEG (3 patients) and scalp EEG (2 patients) recordings were collected. Intracranial EEG recordings were obtained from epileptic patients with bilaterally, surgically implanted microelectrodes in the hippocampus, temporal and frontal lobe cortexes. The EEG signals were recorded using amplifiers with an input range of ±0.6 mV, a frequency range of 0.5-70 Hz and a sampling frequency of 200Hz using an analog-to-digital converter with 10-bit quantization. The EEG signal was filtered using an analog low-pass filter at 70Hz, digital band-pass filter between 0.1-30Hz and notch filter at 60Hz. The multichannel EEG signals (28–32) were obtained from long-term continuous recordings in three patients (6-11.7 days). Fig. 4.1(a) shows the electrode placement for the intracranial recordings.

Scalp EEG recordings with 21 recording electrodes (according to general technical standards) were obtained from 2 epileptic patients. The recording electrodes were placed according to the international 10-20 system as shown in Fig. 4.1(b). Additional electrodes were placed between the standard electrodes as proposed by the American Clinical Neurophysiology Society. The sampling frequency was typically chosen to also be 200Hz. An analog low-pass filter with 70Hz cutoff with digital band-pass filter between 0.1-30Hz and notch filter at 60Hz were used. The obtained recording was around 12hrs in duration for each patient. The long-term EEG recordings from five epileptic patients were obtained

to evaluate the performance of our proposed seizure detection algorithm. Information on Patient ID, recording duration, type of recording and total number of seizures is given in Table 4.1.

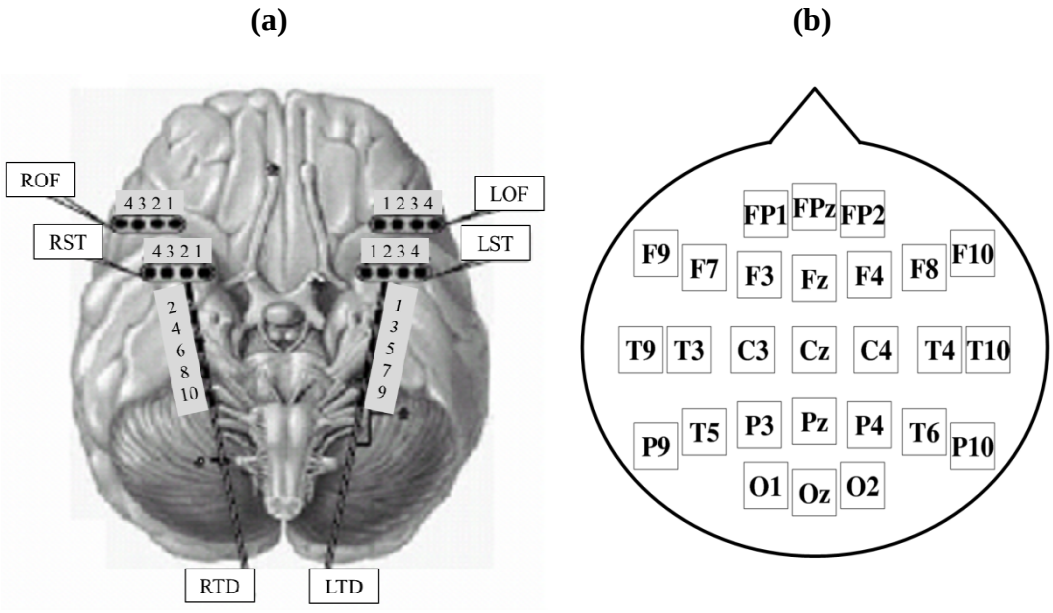

Figure 4.1: Electrode montage for intracranial and scalp EEG recording: (a) Placement of depth and subdural electrodes. Electrode strips placed over the left orbitofrontal (LOF), right orbitofrontal (ROF), left subtemporal (LST) and right subtemporal cortex (RST). Depth electrodes are placed in the left temporal depth (LTD) and right temporal depth (RTD) to record hippocampal EEG activity. (b) Arrangement of electrodes for recording scalp-EEG according to international 10-20 system.

Table 4.1: Patient Data

Patient ID	Recording duration (hrs)	Type of recording	No. of Seizures
1	281.34	Intracranial	7
2	217.94	Intracranial	24
3	145.75	Intracranial	20
4	13.73	Scalp	2
5	12	Scalp	3

4.2 Evaluation Procedure of Seizure Detection Algorithm

The performance of a seizure detection algorithm is measured by using the following criteria:

- True positives

  The number of marked seizures declared as seizure warnings by the seizure detection algorithm.

- False positives

  The number of seizure warnings generated by the seizure detection algorithm which were not seizures (when there was no marked seizure event by the physician).

- False negatives

  The number of missed seizures for which no seizure warning was generated by the seizure detection algorithm.

- Sensitivity

  This is a statistical measure to quantify the ability of the seizure detection algorithm to effectively identify true seizure events. It is given by Eq. 4.1 as

$$Sensitivity = \frac{True\ positives}{True\ positives + False\ negatives} * 100\% \qquad (4.1)$$

- False positive rate per hour (Specificity)

  It is the ratio of the number of false positives generated by the algorithm to the total recording duration (in hours).

  An *"ideal"* seizure detection algorithm would have a sensitivity of 100% with 0 false positives per hour, which would mean that all marked seizure events were correctly identified by the algorithm without generating any false positives.

4.3 Case Analysis: Patient-3

We choose an intracranial long-term EEG recording from a patient with medically intractable epilepsy, admitted to the hospital for detection of epileptogenic focus and possible resective surgery, to present a full-scale analysis of our seizure detection algorithm. The electrode placement was similar to Fig. 4.1(a). 25 out of the 28 recording electrodes were used in our analysis, as 3 electrodes had recording problems and were excluded. For a recording duration of 145.75 hours, a total of 20 epileptic seizures were documented in the patient report, with 9 subclinical seizures and 11 typical complex partial seizures.

Our seizure detection algorithm detected 19 out of the 20 seizures (sensitivity 95%) with 0.0207 false detections per hour. The performance of the algorithm was evaluated using the sensitivity and the number of false detections per hour for different combinations of threshold values (Th_1 and Th_2) and is shown in Fig. 4.2. The combination of thresholds giving the best performance in terms of both sensitivity and false detections per hour (marked in green) was found to be for Th_1 = 5 and Th_2 = 3.5. For the threshold chosen in our algorithm, (Th_1 = 5 and Th_2 = 3), sensitivity was found to be the same as the optimal at 95% with a small increase in the number of false positives per hour from 0.0069 to 0.0207 (marked in black). The missed seizure was found to be of duration of only around 10sec as shown in Fig. 4.3, that is, of duration close to the resolution of our algorithm in its current form, which is not typical for seizures and should be considered as a difficult seizure to be captured by the seizure detection algorithm. The difference in the performance of the used threshold values versus the optimal ones is small and can thus be claimed that the proposed algorithm is pretty robust.

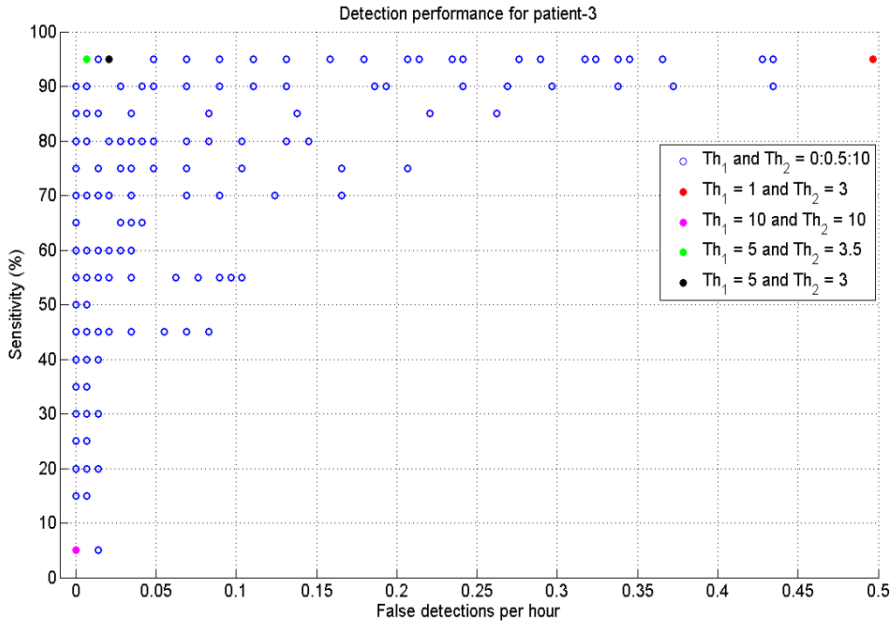

Figure 4.2: Performance (ROC) of seizure detection algorithm for different combination of thresholds Th_1 and Th_2 (in blue). The green dot marks the best performance. The black dot marks the performance for the threshold selected in our algorithm. The magenta and red dots correspond to cases of worst performance, producing respectively 5% sensitivity and 0 false positives per hour and 95% sensitivity with 1 false positive every 2 hours.

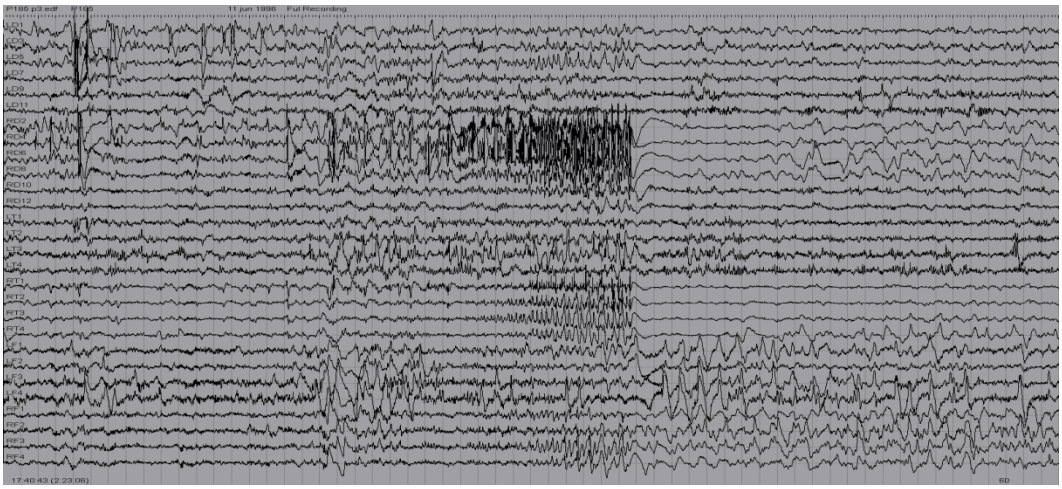

Figure 4.3: 60sec of EEG with a subclinical seizure missed by our detection algorithm (Patient-3).

4.4 Results

The corresponding results from running our seizure detection algorithm on the EEG from all five epileptic patients are given in Table 4.2. The sensitivity ranged from 85.71% to 100%, while the false positive rate per hour ranged from 0 to 1 every 6.5 hours. The average sensitivity for seizure detection across all 5 patients was 93.64% with an average specificity of 0.0484 false positives per hour.

Interestingly, the best results sensitivity-wise were obtained from the scalp recordings (100% in both scalp-EEG patients), but for one of them (patient 5) we had the worst specificity of 0.154, almost 3 times larger than the worst for intracranial recordings. This is indicative of the quality of scalp EEG recordings and their susceptibility to recording artifacts. Lastly, we should note here that the majority of missed seizures in the intracranial recordings were of small duration. The seizure missed in Patient-1 and Patient-3 were subclinical events having EEG

duration of less than 10sec. The 3 seizures missed in Patient-2 were localized to a specific region of brain having EEG duration of less than 10sec.

Table 4.2: Performance of Seizure Detection Algorithm

Patient ID	True positives	False positives	Sensitivity (%)	False positives / hr
1	6	12	85.71	0.04
2	21	6	87.5	0.027
3	19	3	95	0.021
4	2	2	100	0.154
5	3	0	100	0
TOTAL/ AVERAGE	**51**	**23**	**93.64**	**0.0484**

4.5 Full Comparison

The seizure detection algorithm uses two measures, with two different thresholds (e.g. Th_1=5 and Th_2=3). In this cascade arrangement, the order of the use of the measures could affect the performance of the algorithm. To evaluate the performance of the algorithm with a different order, the sequence of the steps where each measure is evaluated was interchanged. We also tested an additional frequency-based measure, earlier used for seizure detection (Temko, Nadeu, Marnane, Boylan, & Lightbody, 2011). An additional motivation for this was the dependence our measures have (by construction) to the frequency content of the EEG. We wanted to test if this dependency is a primary factor for our seizure detection algorithm's performance. The "purely" frequency measure we used was

the maximum energy in 8 sub-band frequencies (2-3Hz, 3-4Hz, …., 9-10Hz) and we denote it by $F_{max.}$

Results from the exhaustive comparison of performance of the seizure detection algorithm for different combinations of these 3 features (STL_{max},TE and F_{max}) are given in Table 4.3. The seizure detection algorithm was considered to have 2 outlier detection blocks as before, with block-1 identifying the candidate EEG segments S_i for having seizure-like activity and block-2 checking whether these candidate segments S_i pass the condition of the second block and be finally asserted as a seizure. The thresholds Th_1=5 and Th_2=3 for block-1 and block-2 respectively were retained for all combinations of selected features.

Our detailed analysis on 5 epileptic patients using mean sensitivity and mean specificity in terms of false positives/hr shows that the combination of $ASTL_{max}$ and ATE in block-1 and block-2 respectively performed the best, giving a mean sensitivity of 93.64% with a mean specificity of 0.049 false positives/hr. Other combinations provided better specificity, but at the expense of sensitivity (e.g. $ASTL_{max}$ in block-1 and a combination of ATE--F_{max} in block-2; specificity 0.0208, sensitivity 67.88%). No other combination had better sensitivity than the original order of blocks depicted in Fig. 3.2. It is also very interesting that use of $ASTL_{max}$ alone in block-1 and omitting block-2 provides the same sensitivity, but with a huge reduction in specificity (almost 20 times worse), a fact that validates both the usefulness of the second block, and the complementary nature of the two measures for a good seizure detection performance.

Table 4.3: Performance of seizure detection algorithm for different combination of features for Patient-3 (Intracranial EEG recording) with mean performance across patients.

	Patient - 3		**Across 5 Patients**	
Features	**Sensitivity (%)**	**False positives/hr**	**Mean Sensitivity (%)**	**Mean false positives/hr**
T -- L & F*	85	0.014	49.2619	0.0839
T -- L | F	95	0.103	65.7857	0.4510
F -- L & T	80	0.021	46.4762	0.0412
F -- L | T	85	0.186	59.9762	0.3662
L -- T & F	90	0	67.8809	0.0208
L -- T | F	95	0.028	93.6429	0.0655
L -- T	**95**	**0.021**	**93.6429**	**0.0490**
L -- F	90	0.007	67.8809	0.0372
T -- F	95	0.103	62.9286	0.4406
F -- T	85	0.172	59.9762	0.3295
T -- L	90	0.014	53.1190	0.1199
F -- L	80	0.041	46.4762	0.0868
T	95	0.2396	76.1429	0.9060
F	85	0.1982	66.6429	0.6170
L	95	0.5945	93.6429	0.7210

*where T -- L&F denotes that the feature used in the block-1 was ATE followed by a logical 'AND' condition between features $ASTL_{max}$ and F_{max} in block-2, while T – L | F denotes a logical 'OR' condition in block-2. Similarly for the rest of the entries in the first column.

Chapter 5

CONCLUSION

The motivation for the development of an automated seizure detection algorithm in this MS research was to assist physicians in the laborious, time consuming and expensive task of seizure detection from long-term EEG recordings. Within this framework, we developed and tested a new seizure detection algorithm based on measures from linear and nonlinear dynamics, i.e., the adaptive short-term maximum Lyapunov exponent (ASTLmax) and the adaptive Teager energy (ATE). The algorithm was tested on long-term (0.5-11.7 days) continuous EEG recordings from five patients (3 with intracranial and 2 with scalp EEG) and a total of 56 seizures, producing a mean sensitivity of 93% across all seizures and mean specificity of 0.048 false positives per hour. The developed seizure detection algorithm is data-adaptive, training-free and patient-independent. It is expected that this algorithm lead to faster and more accurate diagnosis, better evaluation of treatment, and possibly to better treatments if it is incorporated on-line and real-time with advanced neuromodulation therapies for epilepsy.

REFERENCES

Abarbanel, H. D. I. (1996). *Analysis of observed chaotic data* Springer Verlag.

Adeli, H., Ghosh-Dastidar, S., & Dadmehr, N. (2007). A wavelet-chaos methodology for analysis of EEGs and EEG subbands to detect seizure and epilepsy. *Biomedical Engineering, IEEE Transactions on, 54*(2), 205-211.

Baker, G. A., Jacoby, A., Buck, D., Stalgis, C., & Monnet, D. (1997). Quality of life of people with epilepsy: A european study. *Epilepsia, 38*(3), 353-362.

Başar, E. (1980). *EEG-brain dynamics: Relation between EEG and brain evoked potentials* Elsevier-North-Holland Biomedical Press.

Benettin, G., Galgani, L., Giorgilli, A., & Strelcyn, J. M. (1980). Lyapunov characteristic exponents for smooth dynamical systems and for hamiltonian systems; a method for computing all of them. part 1: Theory. *Meccanica, 15*(1), 9-20.

Brazier, M. A. B. (1961). *A history of the electrical activity of the brain: The first half-century* Oxford, England: Macmillan.

Casdagli, M. C., Iasemidis, L. D., Savit, R. S., Gilmore, R. L., Roper, S. N., & Chris Sackellares, J. (1997). Non-linearity in invasive EEG recordings from patients with temporal lobe epilepsy. *Electroencephalography and Clinical Neurophysiology, 102*(2), 98-105.

Casdagli, M., Iasemidis, L., Sackellares, J., Roper, S., Gilmore, R., & Savit, R. (1996). Characterizing nonlinearity in invasive EEG recordings from temporal lobe epilepsy. *Physica D: Nonlinear Phenomena, 99*(2-3), 381-399.

Choi, J., & Kim, T. (2002). Neural action potential detector using multi-resolution TEO. *Electronics Letters, 38*(12), 541-543.

Dubuc, B., Quiniou, J., Roques-Carmes, C., Tricot, C., & Zucker, S. (1989). Evaluating the fractal dimension of profiles. *Physical Review A, 39*(3), 1500.

Fisch, B. J. (2003). *Fisch and spehlmann's EEG primer* Elsevier.

Fisher, R. S., Boas, W. E., Blume, W., Elger, C., Genton, P., Lee, P., & Engel Jr, J. (2005). Epileptic seizures and epilepsy: Definitions proposed by the international league against epilepsy (ILAE) and the international bureau for epilepsy (IBE). *Epilepsia, 46*(4), 470-472.

Franaszczuk, P. J., Bergey, G. K., Durka, P. J., & Eisenberg, H. M. (1998). Time-frequency analysis using the matching pursuit algorithm applied to seizures originating from the mesial temporal lobe. *Electroencephalography and Clinical Neurophysiology, 106*(6), 513-521.

Gabor, A., Leach, R., & Dowla, F. (1996). Automated seizure detection using a self-organizing neural network. *Electroencephalography and Clinical Neurophysiology, 99*(3), 257-266.

Gotman, J. (1982). Automatic recognition of epileptic seizures in the EEG. *Electroencephalography and Clinical Neurophysiology, 54*(5), 530-540.

Gotman, J. (1990). Automatic seizure detection: Improvements and evaluation. *Electroencephalography and Clinical Neurophysiology, 76*(4), 317-324.

Haken, H. (1996). Principles of brain functioning:(a synergetic approach to brain activity, behavior and cognition) Springer.

Hastings, A., & Powell, T. (1991). Chaos in a three-species food chain. *Ecology,* , 896-903.

Iasemidis, L. D., Chris Sackellares, J., Zaveri, H. P., & Williams, W. J. (1990). Phase space topography and the lyapunov exponent of electrocorticograms in partial seizures. *Brain Topography, 2*(3), 187-201.

Iasemidis, L. D., Olson, L. D., Savit, R. S., & Sackellares, J. C. (1994). Time dependencies in the occurrences of epileptic seizures. *Epilepsy Research, 17*(1), 81-94.

Iasemidis, L. D., & Sackellares, J. C. (1991). The evolution with time of the spatial distribution of the largest lyapunov exponent on the human epileptic cortex. *Measuring Chaos in the Human Brain,* , 49-82.

Iasemidis, L. D., Shiau, D. S., Chaovalitwongse, W., Sackellares, J. C., Pardalos, P. M., Principe, J. C., . . . Tsakalis, K. (2003). Adaptive epileptic seizure prediction system. *Biomedical Engineering, IEEE Transactions on, 50*(5), 616-627.

Iasemidis, L., Principe, J., Czaplewski, J., Gilmore, R., Roper, S., & Sackellares, J. (1997). Spatiotemporal transition to epileptic seizures: A nonlinear dynamical analysis of scalp and intracranial EEG recordings. *Spatiotemporal Models in Biological and Artificial Systems,* , 81-88.

Iasemidis, L., Principe, J., & Sackellares, J. (2000). Measurement and quantification of spatiotemporal dynamics of human epileptic seizures. *Nonlinear Biomedical Signal Processing, 2,* 294-318.

Iasemidis, L., Zaveri, H., Sackellares, J., Williams, W., & Hood, T. (1988). Nonlinear dynamics of electrocorticographic data. *J.Clin.Neurophysiol, 5,* 339.

Ives, J., & Woods, J. (1980). A study of 100 patients with focal epilepsy using a 4-channel ambulatory cassette recorder. *Proceedings of the Third International Symposium on Ambulatory Monitoring(Eds FD Scott. EB Raftery and L. Goulding). London. Academic Press,* 383-392.

Kaiser, J. F. (1993). Some useful properties of teager's energy operators. *Acoustics, Speech, and Signal Processing, 1993. ICASSP-93., 1993 IEEE International Conference on, , 3* 149-152 vol. 3.

Khan, Y., & Gotman, J. (2003). Wavelet based automatic seizure detection in intracerebral electroencephalogram. *Clinical Neurophysiology, 114*(5), 898-908.

Liebovitch, L. S., & Toth, T. (1989). A fast algorithm to determine fractal dimensions by box counting. *Physics Letters A, 141*(8-9), 386-390.

Olson, L., Iasemidis, L., & Sackellares, J. (1989). Evidence that interseizure intervals exhibit low dimensional dynamics. *Epilepsia, 30*, 644.

Osorio, I., Frei, M. G., & Wilkinson, S. B. (1998). Real-time automated detection and quantitative analysis of seizures and short-term prediction of clinical onset. Epilepsia, 39(6), 615-627.

Päivinen, N., Lammi, S., Pitkänen, A., Nissinen, J., Penttonen, M., & Grönfors, T. (2005). Epileptic seizure detection: A nonlinear viewpoint. *Computer Methods and Programs in Biomedicine, 79*(2), 151-159.

Pašić, M. (2003). Minkowski–Bouligand dimension of solutions of the one-dimensional-laplacian. *Journal of Differential Equations, 190*(1), 268-305.

Roux, J. C., Simoyi, R. H., & Swinney, H. L. (1983). Observation of a strange attractor. *Physica D: Nonlinear Phenomena, 8*(1-2), 257-266.

Sabesan, S., Good, L. B., Tsakalis, K. S., Spanias, A., Treiman, D. M., & Iasemidis, L. D. (2009). Information flow and application to epileptogenic focus localization from intracranial EEG. *Neural Systems and Rehabilitation Engineering, IEEE Transactions on, 17*(3), 244-253.

Sackellares, J. C., Iasemidis, L. D., Shiau, D. S., Gilmore, R. L., & Roper, S. N. (2000). Epilepsy—when chaos fails. *Chaos in the Brain,* , 112-133.

Schaffer, W. M. (1985). Order and chaos in ecological systems. *Ecology,* , 93-106.

Shimada, I., & Nagashima, T. (1979). A numerical approach to ergodic problem of dissipative dynamical systems. *Prog.Theor.Phys, 61*(6), 1605-1616.

Swinney, H. L. (1983). Observations of order and chaos in nonlinear systems. *Physica D: Nonlinear Phenomena, 7*(1), 3-15.

Takens, F. (1981). Detecting strange attractors in turbulence. *Dynamical Systems and Turbulence, Warwick 1980,* , 366-381.

Temko, A., Nadeu, C., Marnane, W., Boylan, G., & Lightbody, G. (2011). EEG signal description with spectral-envelope-based speech recognition features for detection of neonatal seizures. *Information Technology in Biomedicine, IEEE Transactions on,* (99), 1-1.

Tucker, W. (1999). The lorenz attractor exists. *Comptes Rendus De l'Académie Des Sciences-Series I-Mathematics, 328*(12), 1197-1202.

Webber, W., Lesser, R. P., Richardson, R. T., & Wilson, K. (1996). An approach to seizure detection using an artificial neural network (ANN). *Electroencephalography and Clinical Neurophysiology, 98*(4), 250-272.

Wolf, A., Swift, J. B., Swinney, H. L., & Vastano, J. A. (1985). Determining lyapunov exponents from a time series. *Physica D: Nonlinear Phenomena, 16*(3), 285-317.